Magnetic susceptibility and thermoelectric power of tungsten intermediary oxides

1994 J. Phys.: Condens. Matter 6 7909

(http://iopscience.iop.org/0953-8984/6/39/011)

J. Phys.: Condens. Matter 6 (1994) 7909–7919. Printed in the UK

Magnetic susceptibility and thermoelectric power of tungsten intermediary oxides

A Polaczek†, M Pękała† and Z Obuszko‡

† Department of Chemistry, University of Warsaw, Al. Żwirki i Wigury 101, PL-02-089 Warsaw, Poland

‡ Institute of Electronics, Academy of Mining and Metallurgy, Al. Mickiewicza 30, Cracow, Poland

Received 18 February 1994, in final form 4 May 1994

Abstract. The magnetic susceptibility of the tungsten intermediary oxides WO_{3-x} ($0.05 \leqslant x \leqslant 0.28$) with the crystal shear and pentagonal column structures was measured using the Faraday method. A feeble temperature-independent paramagnetic component $\chi(e)$ of the total susceptibility was present in each case. Using the Pauli–Peierls–Landau formula, the values of the effective mass were calculated. The ratio m^*/m was in the range 1.1–1.55 except for $WO_{2.833}(W_{24}O_{68})$, where this value was as large as 4.0. Measurements of the thermoelectric power Q confirm generally the metallic character of the oxides, but the Q versus temperature dependence in the range 20–280 K is more complicated as in the case of tungsten bronzes. Superconductivity was not detected down to 1.5 K.

1. Introduction

The effect of non-stoichiometry on the properties of transition-metal oxides is of particular interest in cases where the stoichiometric compound is non-conducting and diamagnetic, and the lattice can accommodate a considerable deficit of oxygen; WO_3 is a known example. This oxide is of special interest as it forms the basis of tungsten bronzes (TBs). The electronic properties of TBs are related to the oxide matrix conduction band: W $5d(t_{2g})$–O $2p(\pi)$; the role of the donor metal is to supply electrons to this band (cf [1, 2]). The partial loss of oxygen from WO_3 should have similar consequences as the insertion of donors (cf. [3]). However, the reduction of WO_3 is accompanied by structural changes; thus it is not clear whether the model proposed for TBs fits well for WO_{3-x}.

For a low degree of reduction ($x < 0.01$), single oxygen vacancies may be present in WO_{3-x} in a low concentration, but with increasing x the lattice tends to eliminate them by the crystal shear (CS) mechanism; groups of edge-sharing WO_6 octahedra are arranged along some crystallographic planes (shear planes). If the shear planes are isolated or disordered with respect to their directions and/or mutual distances, they can be regarded as extended defects. With further increase in x, the shear planes begin to interact and tend to align parallel; the areas between them are filled with a WO_3-like array of only corner-sharing WO_6. If the shear planes are all parallel and equidistant, a crystalline phase with defined structure arises. All CS phases so far isolated belong to the (103)CS series (the indices refer to the idealized regular WO_3) identical with Magneli's W_nO_{3n-2} series. This structure is presented in figure 1 for $W_{20}O_{58}$. Below $n \simeq 15$ ($x \geqslant 0.13$) the CS structure becomes unstable and further reduction occurs owing to another mechanism involving the formation of SC pentagonal columns (PCs) parallel to the monoclinic b axis. The PCs are either single

0953-8984/94/397909+11$19.50

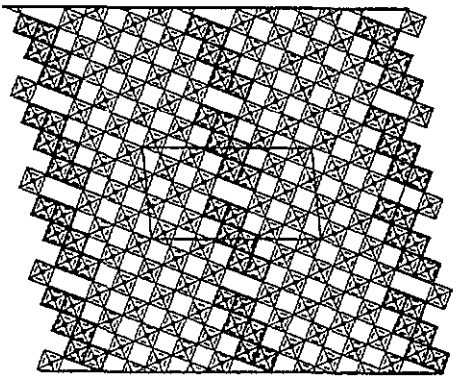

Figure 1. The idealized structure of $W_{20}O_{58}$ (member of the (103)CS series) projected onto the a–c plane. The unit cell is outlined. (After Sundberg [9].)

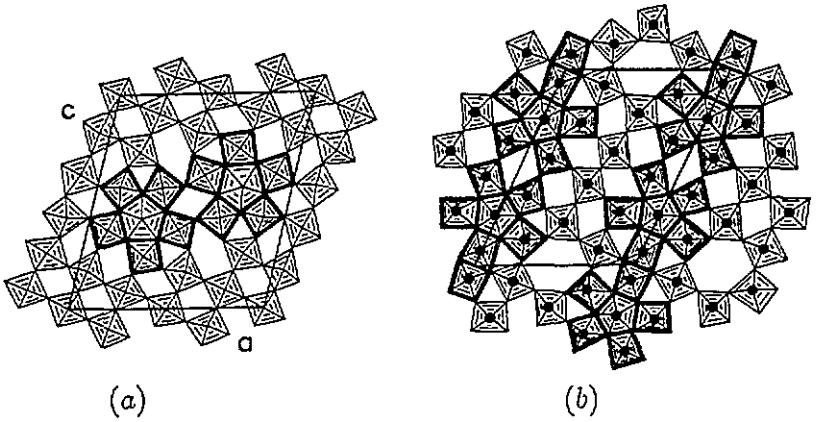

Figure 2. The idealized structure of (*a*) $W_{24}O_{68}$ and (*b*) $W_{18}O_{49}$ projected onto the a–c plane. The polyhedra forming PCS are shaded. (After Sundberg [9, 35].)

or paired by edge sharing (PC–PC). Two PC oxides have been identified: $W_{18}O_{49}$ and $W_{24}O_{68}$ (figure 2). A detailed description of CS and PC structures has been given in [4–8, 12]. In the following we refer to these phases as to the tungsten intermediary oxides (TIOs). Their common feature is that layers formed by only corner-sharing WO_6 alternate with the 'dense' layers, where the octahedra are partially edge sharing. $W_{18}O_{49}$ is the last member of the TIO series, as no other oxide exists in the $WO_{2.7}$–WO_2 region (for the W–O diagram see [9, 10]). $W_{18}O_{49}$ has a narrow homogeneity range and can be isolated in a pure form. This is, however, not the case for other TIOs, where even very prolonged heating does not yield a single-phase product (see [10, 11]).

Some 40 years ago, Magnèli observed the metallic properties of $W_{20}O_{58}$ and $W_{18}O_{49}$. Later it was confirmed by thermopower [3, 15] and electrical conductivity [16, 17] measurements. Tilley [18] considered the importance of the high dielectric constant of WO_3 for the formation and stability of CS structures. The magnetic susceptibility of WO_{3-x} was investigated by Sienko and Banerjee [19]; Pauli-type paramagnetism was found. However, they paid no attention to the phase composition of their samples and considered WO_{3-x} as a random solution of anionic vacancies in the WO_3 lattice. In the present study we

have examined the magnetic properties as well as the thermoelectric power of CS- and PC-type TIOs in order to verify the applicability of the electron gas model, and to see whether structural factors play an important role or not.

2. Experimental details

2.1. Preparation and x-ray investigations

Oxides of a definite mean composition WO_{3-x} were obtained by the solid state reaction $(x/3)W + (1-x/3)WO_3 = WO_{3-x}$. Aldrich reagents 99.995% WO_3 and 99.99% tungsten powder (less than 10 μm) were used. The reagents were ground in an agate mortar and, after prolonged pumping, sealed off in a quartz ampoule. the reaction was carried out in two steps: in the first step the mixture was heated at 1000 °C for 2 d. The product was then thoroughly ground in a dry nitrogen atmosphere, pressed in pellets and repeatedly heated *in vacuo* at 1120 °C for 3 weeks; care was taken to reduce the temperature gradient as much as possible. Subsequently the temperature was lowered slowly to 960 °C, where the sample was rapidly cooled. Finally the product was ground and mixed. The average composition was checked by heating a known amount of the substance in air until a constant weight was achieved. The value x_g determined from the mass increment was compared with the stoichiometric value x, and agreement within the limits $\pm 2\%$ was stated. Densities were measured pycnometrically using water as the immersion liquid, with an accuracy of ± 0.015 g cm^{-3}.

All substances were checked by the x-ray powder method and the results were compared with the published data (for references see table 1). In the case of $WO_{2.722}$, pure $W_{18}O_{49}$ was found. The spectrum for $WO_{2.833}$ agreed well with the data of Booth *et al* [10], showing that $W_{24}O_{68}$ was the main component. $WO_{2.90}$ gave a clear spectrum with unbroadened peaks, which could be fitted using the $W_{20}O_{58}$ lattice constants given by Magnèli. The diffraction patterns of the other oxides were rather difficult to interpret. There was an unquestionable analogy between $WO_{2.92}$ and $WO_{2.90}$ but in the first case the peaks were considerably broadened, possibly as a result of Wadsley-type defects. The same was true for $WO_{2.875}$ but, moreover, a small admixture of an unidentified phase was present. Interpretation of the $WO_{2.95}$ spectrum was hindered because of its complicated character; the oxide was certainly not identical with $W_{40}O_{118}$ described by Gadò and Magnèli [23] and presented probably a mixture of various members of the (103)CS and (102)CS homologous series.

In table 1, some structural and physical data relevant to the TIOs are given. The 'molar weight' refers to the WO_{3-x} formula unit; the molar volume is calculated as M/d_c, using crystallographic densities. N_{ex} represents the number of excess electrons per WO_{3-x} mole, defined as twice the number of oxygen atoms removed from the WO_3 lattice.

2.2. Magnetic measurements

Magnetic susceptibilities were measured using an automatic compensation Faraday balance. Pressed samples of cylindrical form and constant volume (0.2 cm^3) were placed within a thin-walled Teflon holder. Shaped pole pieces provided a uniform force field in an area large enough to eliminate effects due to possible small displacements. Mohr's salt was used as standard, taking $\chi = 32.8 \times 10^{-6}$ emu g^{-1} (at 294.3 K). We have tested the whole measurement procedure by using two appropriate reference compounds: stoichiometric WO_3 (the reagent used for synthesis); sodium bronze Na_xWO_3 with $x = 0.70 \pm 0.01$ obtained by the solid state reaction [39] from Specpure reagents and proved by the x-ray method to

Table 1. Structural and physicochemical data for the intermediary tungsten oxides.

Composition (unit-cell formula)	Molar weight	Structural type (space group)	Density (g cm^{-3}) Pycnometric d_p	Density (g cm^{-3}) Crystallographic d_c	Number of excess electrons per mole $N_{ex} \times 10^{-23}$	References
$WO_{2.95}(W_{40}O_{118})$	231.65	(103)CS ($P2$)	7.06	7.13	0.60	[22, 23]
$WO_{2.92}(W_{25}O_{73})$	230.57	(103)CS ($P2$)	7.105	7.11	0.96	[11]
$WO_{2.90}(W_{20}O_{58})$	230.25	(103)CS ($P2/m$)	7.15	7.165	1.20	[10, 13]
$WO_{2.875}(W_{16}O_{46})$	229.85	103(CS) ($P2$)	7.16	—	1.50	[9]
$WO_{2.833}(W_{24}O_{68})$	229.18	PC ($P2$)	7.565	7.60	2.01	[10, 20, 21]
$WO_{2.722}(W_{18}O_{49})$	227.40	PC–PC ($P2/m$)	7.64	7.70	3.35	[10, 14, 16, 17]

be a pure cubic phase. We obtained at room temperature $\chi(WO_3) = -(0.058 \pm 0.0055) \times 10^{-6}$ emu g^{-1} and $\chi(Na_{0.70}WO_3) = (0.027 \pm 0.006) \times 10^{-6}$ emu g^{-1}. This may be compared with the data reported by Greiner *et al* [24]: $-(0.060 \pm 0.005) \times 10^{-6}$ emu g^{-1} and $(0.033 \pm 0.004) \times 10^{-6}$ emu g^{-1} for WO_3 and $Na_{0.694}WO_3$, respectively. For each substance, seven to nine independent measurements were made. Calibration was performed at the beginning and the end of each series; the empty sample holder was checked as well. Nevertheless, owing to the small forces involved, the relative error was rather considerable and, in the case of the oxides $WO_{2.90}$ and $WO_{2.875}$ for which the diamagnetic and paramagnetic components nearly compensate each other, it was large (table 2). It should be noted, however, that the only quantity which is of real interest to us is the difference $\chi - \chi(WO_3)$ (see equation (1) in section 4).

Table 2. Magnetic susceptibility data and calculated effective electron mass for the WO_{3-x} samples investigated.

Formula WO_{3-x}	Molar Volume V (cm^3)	Magnetic susceptibility $\times 10^6$ (emu mol^{-1}) Total χ	Electron, χ(e)	Concentration of excess electrons $(N_{ex}/V) \times 10^{-21}$	Effective mass m^*/m
WO_3	32.4	-13.45 ± 1.27	—	—	1.5–3.2 [3]
$WO_{2.95}$	32.405	-6.01 ± 1.05	6.95	1.86	1.1
$WO_{2.92}$	32.43	-4.84 ± 0.92	7.83	2.97	1.07
$WO_{2.90}$	32.135	-2.30 ± 0.88	10.17	3.75	1.2
$WO_{2.875}$	32.10	2.30 ± 0.94	14.525	4.68	1.45
$WO_{2.833}$	30.155	37.36 ± 1.30	49.17	6.66	4.0
$WO_{2.722}$	29.53	8.64 ± 1.22	19.37	11.34	1.55

ESR experiments were performed with a standard X-band spectrometer (SE/X 2547 type). The samples were mixed and thoroughly ground with WO_3 to reduce the dielectric losses.

2.3. Electrical measurements

Sintered samples of dimensions 3.5 mm × 4.0 mm × 6.5 mm were used. For thermoelectric power investigations the differential method was used. A temperature gradient (2–3 K) was created by a small heater (3–40 mW) thermally connected to one end of the sample, while the opposite end was in direct thermal contact with the cryostat. The temperature was monitored with copper–constantan thermocouples. Corrections were made to account for the thermoelectric power of the copper electrodes. The temperature difference between the sample ends could be measured with an accuracy of 0.05 K and the probable error of thermopower values was ± 0.3 μV K^{-1}. Each run included 100–120 individual points.

3. Results

The measured molar susceptibilities χ (i.e. susceptibilities per gram formula weight WO_{3-x}) are given in table 2. It is of interest to compare our results with those reported by Sienko and Banerjee [19]. They obtained $\chi(WO_{2.75}) = 4.06 \times 10^{-6}$ emu mol^{-1}, $\chi(WO_{2.87}) = -7.11 \times 10^{-6}$ emu mol^{-1} and $\chi(WO_3) = -21.0 \times 10^{-6}$ emu mol^{-1}. It is seen that the values obtained by Sienko and Banerjee are shifted against ours by about 7×10^{-6} emu mol^{-1} downwards. Greiner *et al* [24], who obtained $\chi(WO_3) = -13.9 \times 10^{-6}$ emu mol^{-1} (in very good agreement with our result), pointed out that an incorrect calibration was probably the

reason for this discrepancy. However, so far, as only the difference $\chi(WO_{3-x}) - \chi(WO_3)$ is considered, our results are in reasonable agreement with the data of Sienko and Banerjee. Supplementary experiments for $WO_{2.722}$, $WO_{2.833}$ and $WO_{2.90}$ did not reveal any significant difference between the susceptibilities at room temperature and those at 110 K. No dependence on the magnetic field up to 10 kG could be detected.

No ESR signals were observed at room temperature nor at 78 K. Assuming a rather broad W^{5+} signal of 20 G width and a sensitivity of at least 1×10^{11} spins in a sample containing about 4×10^{20} W atoms, we obtain a W^{5+}-to-W^{6+} ratio of less than 1×10^{-7}. The existence of localized W^{5+} centres can also be excluded (cf [40]).

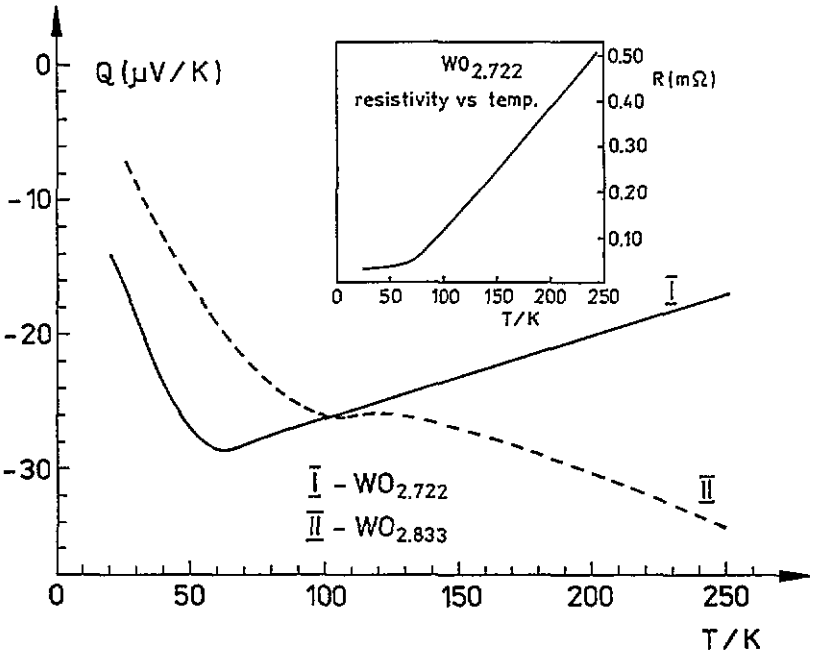

Figure 3. The thermoelectric power versus temperature plot for $WO_{2.722}$ (curve I) and $WO_{2.833}$ (curve II). The inset shows a resisitivity versus temperature plot for $WO_{2.722}$.

The thermoelectric power Q was negative for all samples in the whole 20–280 K range. Absolute values of Q varied from several to several tens of microvolts per kelvin. Figures 3 and 4 present Q versus T plots for $WO_{2.722}$ (curve I), $WO_{2.833}$ (curve II), $WO_{2.90}$ (curve III) and $WO_{2.95}$ (curve IV). In all cases the low-temperature branch of the $Q(T)$ curve (below about 50 K) follows an approximate $\sim T$ law. However, if the whole temperature range is considered, the CS oxides show a different Q versus T dependence from the PC oxides. In the first case the absolute value of Q rises gradually with increasing temperature and a lower oxygen deficit leads to a higher absolute Q. For $WO_{2.722}$, on the other hand, a deep minimum is observed at 60 K followed by an almost linear decrease in the absolute value of Q with increasing temperature. In the case of $WO_{2.833}$, only a weak and diffuse minimum appears at about 105 K and then the absolute value of Q rises again.

The 'specific resistivities' ρ of our sintered samples at room temperature varied from 0.21×10^{-3} Ω cm for $WO_{2.722}$ to 0.25 Ω cm for $WO_{2.95}$. For samples with a lower oxygen deficit the sinters were brittle and the sintering procedure had a considerable effect

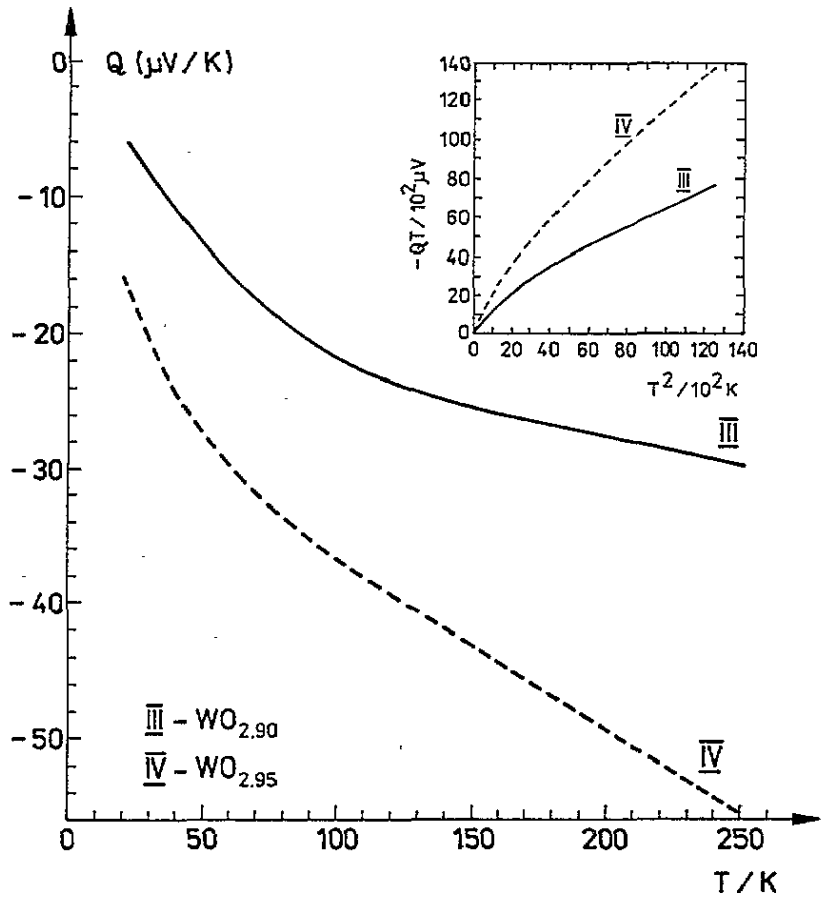

Figure 4. The thermoelectric power versus temperature plot for $WO_{2.90}$ (curve III) and $WO_{2.95}$ (curve IV). The inset shows the same plots in the QT versus T^2 coordinate system.

on ρ probably owing to intergrain contacts. The PC oxides, particularly $W_{18}O_{49}$, behaved in a different manner; very compact sinters could be easily obtained and various samples exhibit relatively small differences of ρ ($\pm 25\%$). The ρ versus T plot is shown in the inset of figure 3 and it is seen that it is linear over a wide temperature range. For the best-conducting sample we obtained $\rho_{RT} = 200\ \mu\Omega$cm and $d\rho/dT = 2.5\ \mu\Omega$ cm K^{-1}. Flux expulsion measurements performed down to 1.5 K did not reveal for any TIO a transition to the superconducting state [37].

4. Discussion

The difference $\chi(WO_{3-x}) - \chi(WO_3)$ has a positive value for all oxides investigated. A decrease in the diamagnetic contribution due to removal of some of the O^{2-} ions can account only for a fraction (of the order of 10%) of this effect. The main part of this paramagnetic shift must be ascribed to excess electrons from the process $O^{2-}_{latt} = \frac{1}{2}O_2(g) + 2e^-_{latt}$. This will be denoted by $\chi(e)$. Both the magnitude of $\chi(e)$ and the absence of the temperature effect show that $\chi(e)$ may be described in terms of Pauli paramagnetism,

in accordance with Sienko's early ideas. There exists, however, no straightforward method of evaluating $\chi(e)$ from the measured susceptibilities. The problem is even more complicated than in the case of TBs, for which the following relation was successfully used: $\chi(M_xWO_3) = \chi(WO_3) + x\chi(M^+) + \chi(e)$ (M ≡ metal) [24]. In the case of WO_{3-x} we shall make two assumptions: firstly we account for the diamagnetism of the removed O^{2-} ions, but the change in the diamagnetic properties of the remaining oxide framework is neglected; secondly the possible contribution from excess electrons which are localized (e.g. as bipolarons) is disregarded. In this case we obtain

$$\chi(e) = \chi(WO_{3-x}) - \chi(WO_3) + x\chi(O^{2-}). \tag{1}$$

Taking $\chi(O^{2-}) = -9.8 \times 10^{-6}$ emu mol^{-1} [19] we have

$$\chi(e) = \chi(WO_{3-x}) + (13.45 - 9.8x) \times 10^{-6} \text{ emu mol}^{-1}. \tag{2}$$

The $\chi(e)$ versus composition diagram is shown in figure 5. The Pauli–Peierls–Landau equation (see e.g. [25]) gives

$$\chi(e)/V = \mu_B^2 g(E_F)(1 - m^2/3m^{*2}). \tag{3}$$

The left-hand side of equation (3) expresses the electron gas susceptibility per cubic centimetre, μ_B is the Bohr magneton, m^* is the effective mass and $g(E_F)$ represents the density of states at the Fermi level per energy unit and cubic centimetre. For a parabolic band populated by n electrons per cubic centimetre, it follows from equation (3) that

$$\chi(e)/V = 4(3\pi^2)^{1/3}(m\mu_B^2/h^2)n^{1/3}[(m^*/m)(1 - m^2/3m^{*2})]. \tag{4}$$

If the electron concentration is known from independent data, m^* will express the influence of structural factors. However, the relation $g(E_F) \sim n^{1/3}$ and hence the correctness of equation (4) may be questioned. For the cubic TB, for example, the parabolic band model gives reasonable but not quite satisfactory results [24, 26]. Specific heat data lead to $g(E_F) \sim n^{\zeta}$ with $\zeta \simeq 1$ [27] which in fact improves the agreement between the experimental and the calculated susceptibilities [24]. Zumsteg [28] obtained the best fit using the Mattheis band calculations combined with specific heat data (see inset of figure 5). This problem was discussed later by Mott [29].

There is no direct information regarding the free-electron concentration in TIOs because of lack of reliable Hall data. For $W_{18}O_{49}$, reflectivity measurements gave $n = 1.9 \times 10^{22}$ cm^{-3} [16] in rough agreement with the calculated value. In view of the absence of localized W^{5+} centres the assumption $n = N_{ex}/V$ has often been made. However, opinions that only 25–50% of the excess electrons were really free were also expressed [3, 30, 34]. We may expect for example that two of the four excess electrons in a (103)CS unit cell form a bipolaron (cf [31]) localized within the sextet of edge-sharing octahedra, giving positively charged clusters $[(W_6O_{16})^{4+}2e^-]$ and free electrons in the WO_3-like layers (cf figure 1). However, the rather large W–W distances within the sextet (3.2–3.3 Å) do not seem to support this hypothesis. Positive evidence is known only in the case of $W_{18}O_{49}$ where a considerable shortening of the W–W distance and the extension of the O–O shared edge in the PC–PC bridge may indicate the formation of an intermetallic bond (cf [16]). Another factor which may be significant is the limitation of the effective volume left to the electrons. We conclude that an effective n^*-value ($n^* < n$) would probably fit equation (4) better.

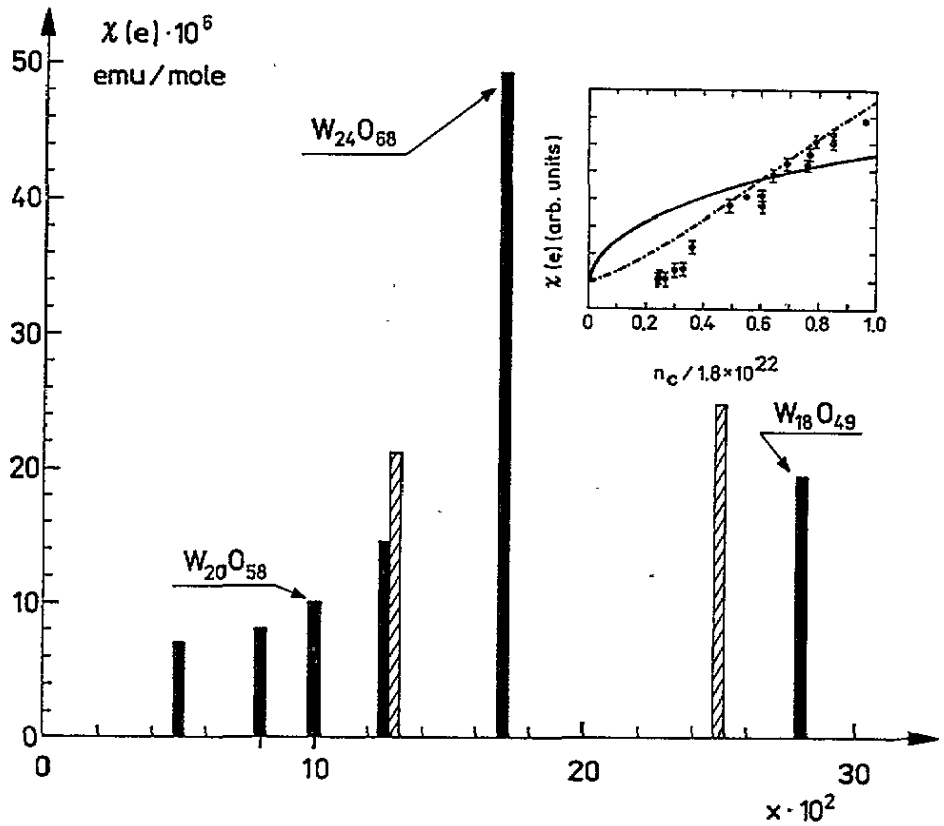

Figure 5. Electron gas susceptibility χ(e) per WO_{3-x} mole versus composition (■). Data from [19] (□) are included for comparison. The inset shows χ(e) versus electron concentration plots for cubic Na_xWO_3: ——, parabolic band; ----, curve calculated by Zemsteg [28].

At the present stage, however, the simplest and most reasonable way is to interpret χ(e) in terms of a uniform electron gas and a parabolic band, assuming that $n = N_{ex}/V$. All possible complicating factors will then influence the values of m^*. The effective masses thus obtained are given in table 2. It is seen that m^*/m varies within rather narrow limits: 1.1–1.55 with some tendency to increase with increasing x. A sharp anomaly is observed only for $WO_{2.833}$ where $m^*/m = 4.0$. It is of interest to compare these values with those reported for TBs. The electron concentration in the metallic TBs is known exactly and reliable magnetic susceptibility data are also given. Cubic Na_xWO_3 was investigated for $0.49 \leqslant x \leqslant 0.89$ which corresponds to $n = (0.9\text{–}1.6) \times 10^{22}$ cm^{-3} [24]. Using the free-electron model the best fit was obtained for $m^*/m = 1.6$. In an earlier study on the Li_xWO_3 and Na_xWO_3 systems Sienko and Truong [32] interpreted the results in terms of a concentration-dependent effective mass: $m^*/m = 1.1\text{–}2.4$. For hexagonal Rb_xWO_3, values in the range 0.84–1.03 were found [33]. It is interesting that electrical methods often give considerably larger m^*/m [3, 26].

The linear temperature dependence of thermopower Q, observed for all oxides below about 50 K, can be explained by the dominant role of the diffusion term Q_d (cf [25]):

$$Q_d = \tfrac{2}{3}(\pi/3)^{2/3}(mk_B^2/e\hbar^2)(m^*/m)n^{-2/3}T. \tag{5}$$

Equation 5 gives reasonable results in the case of metallic TBs [26]. However, for the oxides investigated, the values of Q_d calculated from equation (5) for a given temperature (say, 30 K) using the values of m^*/m and n taken from table 2 are an order of magnitude lower than the measured values. The possibility that, in this temperature range, m^*/m becomes larger (e.g. by the formation of polarons) cannot be excluded; another explanation is that electrons are partially trapped and n is far below N_{ex}/V. Our experimental data show clearly that the $Q \sim n^{-2/3}$ law is not fulfilled in the case of TIOs.

If one considers the Q versus T dependence in the whole temperature range, the phonon drag term Q_{ph} cannot be neglected, of course. On the basis of previous theoretical results, Muhlestein and Danielson [38] have shown in their study on cubic Na_xWO_3 that, for T larger than $\Theta_D/10$, the total Q can be expressed in the form

$$Q = Q_d + Q_{ph} = AT + BT^{-1} \qquad \text{i.e. } QT = B + AT^2. \tag{6}$$

Equation (6) should hold independently of the relative contributions from the N and U processes. In fact, for Na_xWO_3 a linear QT versus T^2 plot was obtained. For the CS oxides the form of the $Q(T)$-function resembles those observed for bronzes; so we have proved whether equation (6) holds also in this case; the QT versus T^2 plots are shown in the inset of figure 4 and it is seen that the departure from linearity is quite considerable. We conclude that the model discussed in [38], which involves constancy of n and m^*, is rather useless in the case of TIOs. The most interesting fact, however, is the appearance of minima on the Q versus T plots in the case of the PC oxides. Particularly significant is the deep minimum at 60 K observed for $W_{18}O_{49}$. There exists some analogy which has been reported for η-Mo_4O_{11} [36], where the existence of CDW instabilities was postulated. More experimental data are needed, however, and we shall not discuss this problem here.

Our electrical resistivity data must be treated with care, as the variation in intergrain contacts with temperature must be taken into account. In the case of $WO_{2.722}$, however, the results may be treated as reliable. The room-temperature specific resistivity is comparable with those reported for small needle-like $W_{18}O_{49}$ crystals [16, 17], and the resistivity ratio $\rho(20\text{ K})/\rho(\text{RT})$ is below 0.1 (see inset of figure 3). The ρ versus T plot is linear over a wide range and the whole $\rho(T)$ curve is of Grüneisen form. We may note that a very similar ρ versus T dependence was reported for the tunnel-type bronzes, Rb_xWO_3 and Tl_xWO_3 [42], and recently for vanadium dioxide above the insulator–metal transition point. [41].

5. Conclusions

The simple quasi-free-electron gas model involving all electrons released in the process $O^{2-} = \frac{1}{2}O_2 + 2e^-$, distributed uniformly in the lattice, can account for the observed magnetic susceptibilities of WO_{3-x} rather well, at least beyond 110 K. The effective electron masses m^*/m calculated from the Pauli–Peierls–Landau formula agree with those reported for the TBs (1.0–2.0). Further investigations are needed to explain the large value (4.0) obtained for $W_{24}O_{68}$. Thermopower and electrical resistivity measurements generally confirm the metallic character of TIOs. However, the temperature dependence of thermopower differs considerably from those observed for metallic bronzes. For $W_{18}O_{49}$ and $W_{24}O_{68}$, minima appear on the Q versus T plots, at 60 K and 105 K, respectively; their origin is still unexplained. More information is needed before a satisfactory model of the electronic properties of the WO_{3-x} will be obtained. It is possible that the models for the CS and PC oxides will diverge in some essential points.

Acknowledgments

Support by BST-439/93, Department of Chemistry, Warsaw University is acknowledged.

References

[1] Ferretti A, Rogers D B and Goodenough J B 1965 *J. Phys. Chem. Solids* **26** 2007
[2] Sienko M J 1967 *The Alkali Metals, Spec. Publ.* **22** 429
[3] Berak J M and Sienko M J 1970 *J. Solid State Chem.* **2** 109
[4] Magnèli A 1953 *Acta Crystallogr.* **6** 495
[5] Alpress J G and Gadò 1970 *Cryst. Latt. Defects* **1** 331
[6] Tilley R J D 1978–9 *Chem. Scr.* **14** 147
[7] Cormack A N, Jones Rachel M, Tasker P W and Catlow C R A 1982 *J. Solid State Chem.* **44** 174
[8] Lundberg M, Sundberg M and Magnèli A 1982 *J Solid State Chem.* **44** 32
[9] Sundberg M 1981 *Chem. Commun. Univ. Stockholm* **5**
[10] Booth J, Ekström T, Iguchi E and Tilley R J D 1982 *J. Solid State Chem.* **41** 293
[11] Sundberg M 1976 *Acta Crystallogr.* B **32** 2144
[12] Sundberg M 1980 *J. Solid State Chem.* **35** 120
[13] Magnèli A 1949 *Nova Acta Reg. Soc. Sci. Upsal.* **14** 3
[14] Magnèli A 1949 *Ark. Kemi* **1** 223
[15] Dryzek J, Polaczek A, Pękała M and Rataj R 1992 *J. Phys.: Condens. Matter* **4** 1399
[16] Viswanathan K, Brandt K and Salje E 1981 *J. Solid State Chem.* **36** 45
[17] Sahle W and Nygren M 1983 *J. Solid State Chem.* **48** 15
[18] Tilley R J D 1977 *Nature* **269** 229
[19] Sienko M J and Banerjee B 1961 *J. Am. Chem. Soc.* **83** 4149
[20] Pickering R and Tilley R J D 1976 *J. Solid State Chem.* **16** 247
[21] Sundberg M 1978–9 *Chem. Scr.* **14** 161
[22] Gadò P and Imre L 1965 *Acta Chim. Hung.* **46** 166
[23] Gadò P and Magnèli A 1965 *Acta. Chem. Scand.* **19** 1514
[24] Greiner J D, Shanks H R and Wallace D C 1962 *J. Chem. Phys.* **36** 772
[25] Wilson A H 1954 *The Theory of Metals* (Cambridge: Cambridge University Press)
[26] Shanks H R, Sidles P H and Danielson G C 1963 *Adv. Chem. Ser.* **39** 237
[27] Vest R W, Griffel M and Smith J F 1958 *J. Chem. Phys.* **28** 293
[28] Zumsteg F C 1976 *Phys. Rev.* B **14** 1406
[29] Mott N F 1977 *Phil. Mag.* **35** 111
[30] Allpress J G, Tilley R J D and Sienko M J 1971 *J. Solid State Chem.* **3** 440
[31] Schirmer O F and Salje E 1980 *J. Phys. C: Solid State Phys.* **13** L1067
[32] Sienko M J and Truong T 1961 *J. Am. Chem. Soc.* **83** 3939
[33] Wanlass D R and Sienko M J 1975 *J. Solid State Chem.* **12** 362
[34] Gehlig R, Salje E, Carley A F and Roberts M W 1983 *J. Solid State Chem.* **49** 318
[35] Sundberg M 1978–9 *Chem. Scr.* **14** 161
[36] Inoue M, Ohara S, Horisaka S, Koyano M and Negishi H 1988 *Phys. Status Solidi* b **148** 659
[37] Zalecki R, Polaczek A and Kołodziejczyk A 1994 in preparation
[38] Muhlestein L D and Danielson G C 1967 *Phys. Rev.* **160** 562
[39] Banks E and Wold A 1968 *Prep. Inorg. Reactions* **4** 237
[40] Gazzinelli R and Schirmer O F 1977 *J. Phys. C: Solid State Phys.* **10** L145
[41] Philip A, Wentzovitch R, Schulz W and Canfield P 1993 *Phys. Rev.* B **48** 4359
[42] Aristimuno A, Shanks H R and Danielson G C 1980 *J. Solid State Chem.* **32** 245